

Zero-shot Image-to-Image Translation

Gaurav Parmar¹ Krishna Kumar Singh² Richard Zhang²
Yijun Li² Jingwan Lu² Jun-Yan Zhu¹
¹Carnegie Mellon University ²Adobe Research

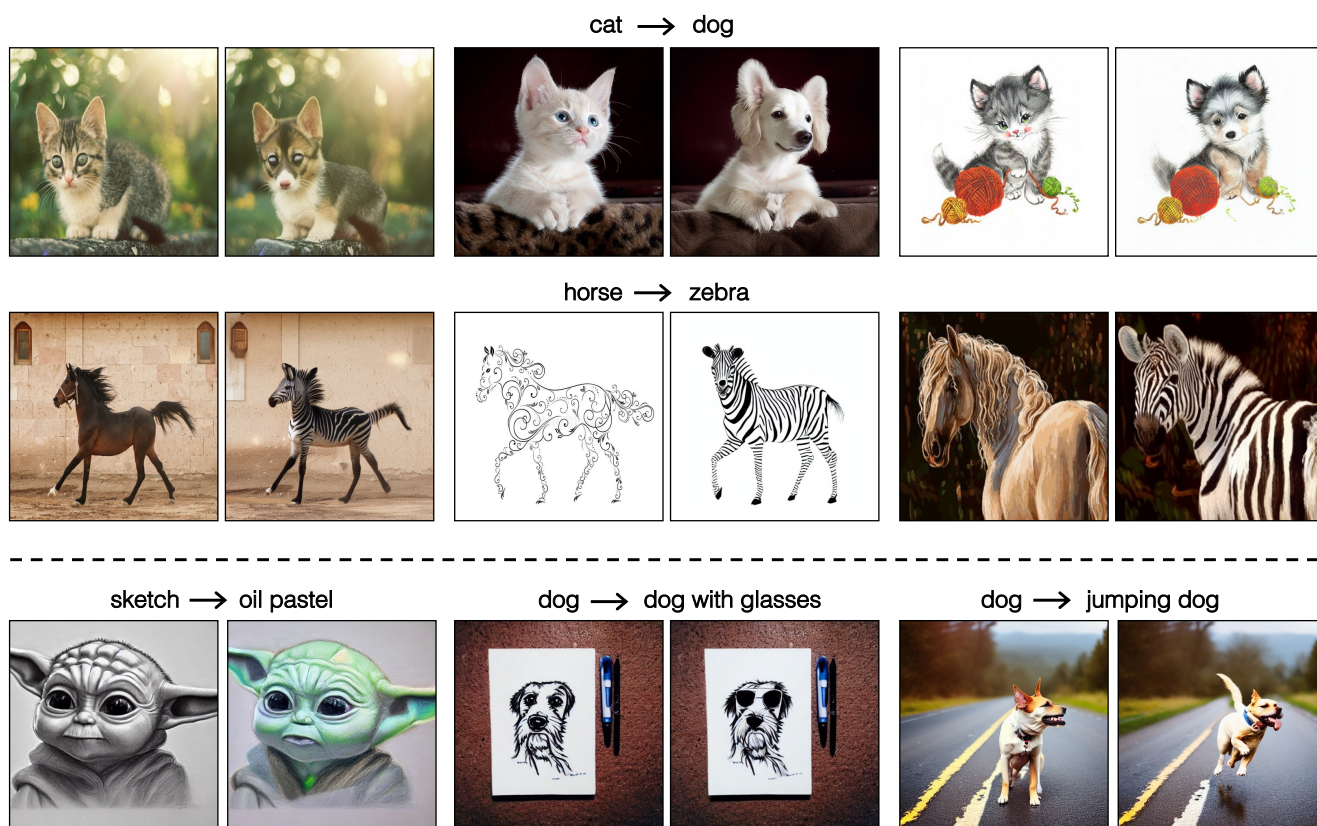


Figure 1: We propose `pix2pix-zero`, a diffusion-based image-to-image translation method that allows users to specify the edit direction on-the-fly (e.g., `cat → dog`). We perform various translation tasks on both real (top 2 rows) and synthetic (bottom row) images, while preserving the structure of the input image. Our method requires *neither* manual text prompting for each input image *nor* costly fine-tuning for each task.

Abstract

Large-scale text-to-image generative models have shown their remarkable ability to synthesize diverse and high-quality images. However, it is still challenging to directly apply these models for editing real images for two reasons. First, it is hard for users to come up with a perfect text prompt that accurately describes every visual detail in the input image. Second, while existing models can introduce desirable changes in certain regions, they often

dramatically alter the input content and introduce unexpected changes in unwanted regions. In this work, we propose `pix2pix-zero`, an image-to-image translation method that can preserve the content of the original image without manual prompting. We first automatically discover editing directions that reflect desired edits in the text embedding space. To preserve the general content structure after editing, we further propose cross-attention guidance, which aims to retain the cross-attention maps of the input image

throughout the diffusion process. In addition, our method does not need additional training for these edits and can directly use the existing pre-trained text-to-image diffusion model. We conduct extensive experiments and show that our method outperforms existing and concurrent works for both real and synthetic image editing.

1. Introduction

Recent text-to-image diffusion models, such as DALL-E 2 [43], Imagen [51] and Stable Diffusion [47] generate diverse and realistic synthetic images with complex objects and scenes, displaying powerful compositional ability. However, repurposing such models for editing *real* images remains challenging.

First, images do not naturally come with text descriptions. Specifying one is cumbersome and time-consuming, as a picture is worth the proverbial “thousand words”, containing many texture details, lighting conditions, and shape subtleties that may not have corresponding words in the vocabulary. Second, even with initial and target text prompts (e.g., changing the word from *cat* to *dog*), existing text-to-image models tend to synthesize completely new content that fails to follow the layout, shape, and object pose of the input image. After all, editing the text prompt only tells us what we want to *change*, but does not convey what we intend to *preserve*. Finally, users may want to perform all kinds of edits on a diverse set of real images. So, we do not want to finetune a large model for each image and edit type due to its prohibitive costs.

To overcome the above issues, we introduce `pix2pix-zero`, a diffusion-based image-to-image translation approach that is *training-free* and *prompt-free*. A user only needs to specify the edit direction in the form of source domain \rightarrow target domain (e.g., *cat* \rightarrow *dog*) on-the-fly, without manually creating text prompts for the input image. Our model can directly use pre-trained text-to-image diffusion models, without additional training for each edit type and image.

In this work, we make two key contributions: (1) *An efficient, automatic editing direction discovery mechanism without input text prompting*. We automatically discover generic edit directions that work for a wide range of input images. Given an original word (e.g., *cat*) and an edited word (e.g., *dog*), we generate two groups of sentences containing the original and edited words separately. Then we compute the CLIP embedding direction between the two groups. As this editing direction is based on multiple sentences, it is more robust than just finding the direction only between the original and edited words. This step only takes about 5 seconds and can be pre-computed. (2) *Content preservation via cross-attention guidance*. Our observation is that the cross-attention map corresponds to the struc-

ture of the generated object. To preserve the original structure, we encourage the text-image cross-attention map to be consistent before and after translation. Hence, we apply the cross-attention guidance to enforce this consistency throughout the diffusion process. In Figure 1, we show various editing results using our method while preserving the structure of input images.

We further improve our results and inference speed with a suite of techniques: (1) Autocorrelation regularization: When applying inversion via DDIM [55], we observe that DDIM inversion is prone to make intermediate predicted noise less Gaussian, which reduces the edibility of an inverted image. Hence, we introduce an autocorrelation regularization to ensure noise to be close to Gaussian during inversion. (2) Conditional GAN distillation: Diffusion models are slow due to the multi-step inference of a costly diffusion process. To enable interactive editing, we distill the diffusion model to a fast conditional GAN model, given paired data of the original and edited images from the diffusion model, enabling real-time inference.

We demonstrate our method on a wide range of image-to-image translation tasks, such as changing the foreground object (*cat* \rightarrow *dog*), modifying the object (adding glasses to a *cat* image), and changing the style of the input (*sketch* \rightarrow *oil pastel*), for both real images and synthetic images. Extensive experiments show that `pix2pix-zero` outperforms existing and concurrent works [35, 22] regarding photo-realism and content preservation. Finally, we include an extensive ablation study on individual algorithmic components and discuss our method’s limitations. See our website <https://pix2pixzero.github.io/> for additional results and the accompanying code.

2. Related Work

Deep image editing with GANs. With generative modeling, image editing techniques have enabled users to express their goals in different ways (e.g., a slider, a spatial mask, or a natural language description). One line of work is to train conditional GANs that translate an input image from one domain to a target domain [28, 52, 71, 14, 61, 26, 39, 34, 5], which often requires task-specific model training. Another category of editing approaches is manipulating the latent space of GANs via image inverting the image and discovering the editing direction [70, 27, 45, 69, 63, 7]. They first project the target image to the latent space of a pretrained GAN model and then edit the image by manipulating the latent code along directions corresponding to disentangled attributes. Numerous prior works propose to finetune the GAN model to better match the input image [8, 38, 46], explore different latent spaces [62, 1, 2], invert into multiple layers [19, 40], and utilize latent edit directions [21, 54, 41, 3]. While these methods are successful on single-category curated datasets, they struggle to obtain

a high-quality inversion on more complex images.

Text-to-Image models. Recently, large-scale text-to-image models have dramatically improved the image quality and diversity by training on an internet-scale text-image datasets [51, 43, 44, 64, 17, 18]. However, they provide limited control over the generation process outside the text input. Editing real images by changing words in the input sentence is not reliable as it often changes too much of the image in unexpected ways. Some methods [37, 4] use additional masks to constrain where edits are applied. Unlike these approaches, our method retains the input structure without any spatial mask. Other recent and concurrent works (e.g., Palette [50], InstructPix2Pix [10], PITI [60]) learn conditional diffusion models tailored for image-to-image translation tasks. In contrast, we use the pre-trained Stable Diffusion models, without additional training.

Image editing with diffusion models. Several recent works have adopted diffusion models for image editing. SDEdit [35] performs editing by first adding noise to the input image together with a user editing guide, and then denoising it to increase its realism. It is later used with text-to-image models such as GLIDE [37] and Stable Diffusion models [47] to perform text-based image inpainting and editing. Other methods [13, 56] propose to modify the diffusion process by incorporating conditioning user inputs but have been only applied to single-category models.

Two concurrent works, Imagic [30] and prompt-to-prompt [22], also attempt structure-preserving editing via pretrained text-to-image diffusion models. Imagic [30] demonstrates great editing results but requires finetuning the entire model for each image. Prompt-to-prompt [22] does not require finetuning and uses the cross-attention map of the original image with values corresponding to edited text to retain structure, with a main focus on synthetic image editing. Our work differs in three ways. First, our method requires no text prompting for the input image. Second, our approach is more robust as we do not directly use the cross-attention map of the original text, which may be incompatible with edited text. Our guidance-based method ensures the cross-attention map of edited images remains close but still has the flexibility to change according to edited text. Third, our method is tailored for real images, while still being effective for synthetic ones. We show that our method outperforms SDEdit and prompt-to-prompt regarding image quality and content preservation.

3. Method

We propose to edit an input image along an *edit direction* (e.g., cat \rightarrow dog). We first invert the input \tilde{x} in a deterministic manner to the corresponding noise map in Section 3.1. In Section 3.2, we present a method for automati-

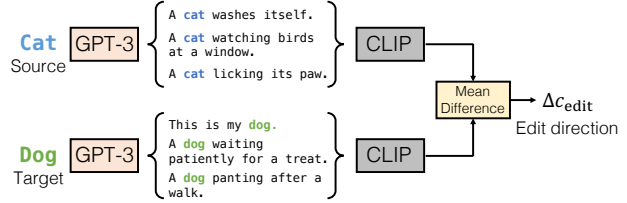


Figure 2: **Discovering edit directions.** Given the source and target text (e.g., cat and dog), we generate a large bank of diverse sentences using GPT-3. We compute their CLIP embeddings and take the mean difference to obtain edit direction Δc_{edit} .

cally discovering and pre-computing edit directions in text embedding space. Applying the edit direction naively often results in unwanted changes in image content. To address this issue, we propose cross-attention guidance that guides the diffusion sampling process and helps retain the input image’s structure (Section 3.3). Note that our method is applicable to different text-to-image models but for this paper we use Stable Diffusion [47] which encodes input image $\tilde{x} \in \mathbb{R}^{X \times X \times 3}$ to latent code $x_0 \in \mathbb{R}^{S \times S \times 4}$. In our experiments, $X = 512$ is the image size, and $S = 64$ is the downsampled latent size. The inversion and editing described in this section happen in the latent space. To invert a text-conditioned model, we generate an initial text prompt c using BLIP [33] to describe the input image \tilde{x} .

3.1. Inverting Real Images

Deterministic inversion. Inversion entails finding a noise map x_{inv} that reconstructs the input latent code x_0 upon sampling. In DDPM [24], this corresponds to the fixed forward noising process, followed by de-noising with the reverse process. However, both the forward and reverse processes of DDPM are stochastic and do not result in a faithful reconstruction. Instead, we adopt the deterministic DDIM [55] reverse process, as shown below:

$$x_{t+1} = \sqrt{\bar{\alpha}_{t+1}} f_{\theta}(x_t, t, c) + \sqrt{1 - \bar{\alpha}_{t+1}} \epsilon_{\theta}(x_t, t, c), \quad (1)$$

where x_t is noised latent code at timestep t , $\epsilon_{\theta}(x_t, t, c)$ is a UNet-based denoiser that predicts added noise in x_t conditional on timestep t and encoded text features c , $\bar{\alpha}_{t+1}$ is noise scaling factor as defined in DDIM [55], and $f_{\theta}(x_t, t, c)$ predicts the final denoised latent code x_0 .

$$f_{\theta}(x_t, t, c) = \frac{x_t - \sqrt{1 - \bar{\alpha}_t} \epsilon_{\theta}(x_t, t, c)}{\sqrt{\bar{\alpha}_t}} \quad (2)$$

We gradually add noise to initial latent code x_0 using DDIM process and at the end of inversion, the final noised latent code x_T is assigned as x_{inv} .

Noise regularization. The inverted noise maps generated by DDIM inversion $\epsilon_{\theta}(z_t, t, c) \in \mathbb{R}^{S \times S \times 4}$ often do not

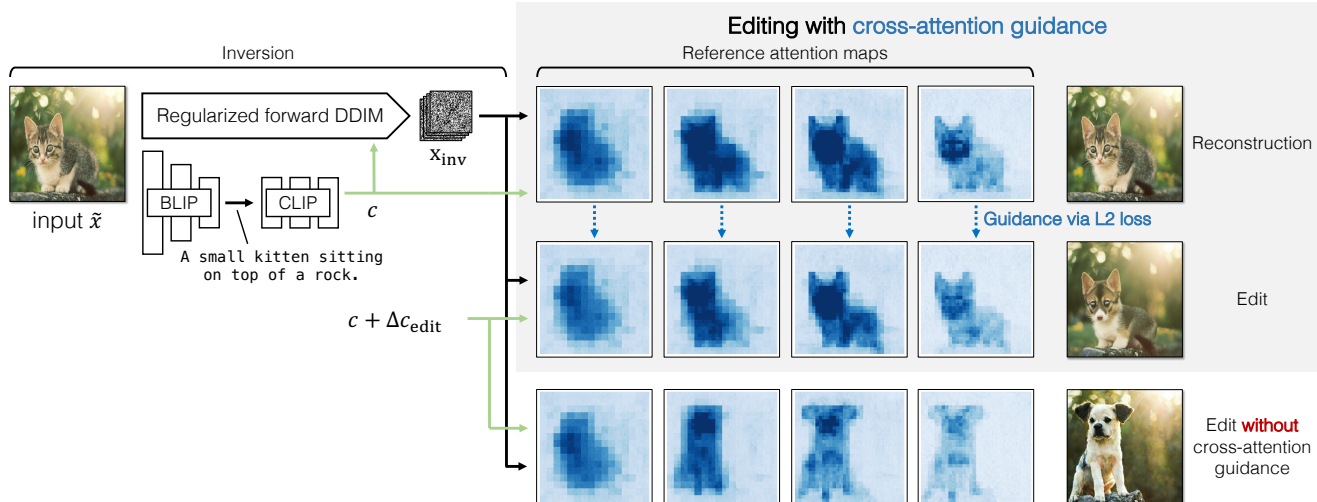


Figure 3: **Overview of the pix2pix-zero method**, illustrated by a cat \rightarrow dog editing example. First, we apply our regularized DDIM inversion to obtain an inverted noise map. This is guided by text embedding c , automatically computed using image captioning network BLIP [33] and the CLIP text embedding model. Then, we denoise with the original text embedding to obtain cross-attention maps, serving as a reference for the input image structure (top row). Next, we denoise with the *edited* text embedding, $c + \Delta c_{\text{edit}}$, using a loss to encourage the cross-attention maps to match the reference cross-attention maps (2nd row). This ensures the structure of edited images does not change dramatically, compared to the original image. Denoising *without* cross-attention guidance is shown in the 3rd row, resulting in large deviations in structure.

follow the statistical properties of uncorrelated, Gaussian white noise, causing poor editability. A Gaussian white noise map should have (1) no correlation between any pair of random locations and (2) zero-mean, unit-variance at each spatial location, which would be reflected in its autocorrelation function being a Kronecker delta function [20]. Following this, we guide the inversion process with an autocorrelation objective, comprised of a pairwise term $\mathcal{L}_{\text{pair}}$ and a KL divergence term \mathcal{L}_{KL} at individual pixel locations.

As densely sampling all pairs of locations is costly, we follow [29] and form a pyramid, where the initial noise level $\eta^0 \in \mathbb{R}^{64 \times 64 \times 4}$ is the predicted noise map ϵ_θ , and each subsequent noise map is average pooled with a 2×2 neighborhood (and multiplied by 2, to preserve the expected variance). We stop at feature size 8×8 , creating 4 noise maps to form set $\{\eta^0, \eta^1, \eta^2, \eta^3\}$.

The pairwise regularization at pyramid level p is the sum of squares of the auto-correlation coefficients at possible δ offsets, normalized over noise map sizes S_p .

$$\mathcal{L}_{\text{pair}} = \sum_p \frac{1}{S_p^2} \sum_{\delta=1}^{S_p-1} \sum_{x,y,c} \eta_{x,y,c}^p \left(\eta_{x-\delta,y,c}^p + \eta_{x,y-\delta,c}^p \right), \quad (3)$$

where $\eta_{x,y,c}^p \in \mathbb{R}$ indexes into a spatial location, using circular indexing, and channel. Note that Karras et al. [29] previously explored using an autocorrelation regularizer for GAN inversion into a noise map. We introduce a few

changes to the autocorrelation idea to boost its performance in the diffusion context: we randomly sample a shift at each iteration, rather than only using $\delta = 1$ as in [29], enabling us to propagate long-range information more efficiently. We hypothesize that in the diffusion context, it is important for each time step to be well-regularized, as relying on multiple iterations to propagate long-range connections causes intermediate time steps to fall out of distribution.

In addition, we find that enforcing the zero-mean unit-variance criteria strictly via normalization [29] leads to divergence during the denoising process. Instead, we formulate this softly as a loss \mathcal{L}_{KL} , as used in variational autoencoders [32]. This enables us to softly balance between the two losses. Our final autocorrelation regularization is $\mathcal{L}_{\text{auto}} = \mathcal{L}_{\text{pair}} + \lambda \mathcal{L}_{\text{KL}}$, where λ balances the two terms.

3.2. Discovering Edit Directions

Recent large generative models allow users to control the image synthesis by specifying a sentence that describes the output image. We instead want to provide the users with an interface where they only need to provide the desired *change* from the source domain to the target domain (e.g., cat \rightarrow dog).

We automatically compute the corresponding text embedding direction vector Δc_{edit} from the source to the target, as illustrated in Figure 2. We generate a large bank of diverse sentences for both source s and the target t , either using an off-the-shelf sentence generator like GPT-3 [11]

or by using predefined prompts around source and target. We then compute the mean difference between CLIP embedding [42] of the sentences. Edited images can be generated by adding the direction to the text prompt embedding. Figure 4 shows the result of several edits, with directions computed using this approach. We find text direction using multiple sentences more robust than a single word and demonstrate this in Section 4. This method of computing edit directions only takes about 5 seconds and only needs to be pre-computed once. Next, we incorporate the edit directions into our image-to-image translation method.

3.3. Editing via Cross-Attention Guidance

Recent large-scale diffusion models [48, 51, 43] incorporate conditioning by augmenting the denoising network ϵ_θ with the cross-attention layer [6, 58]. We use the open-source Stable Diffusion model, built on latent diffusion Models (LDM) [47]. The model produces text embedding c with the CLIP [42] text encoder. Next, to condition the generation on text, the model computes cross-attention between encoded text and intermediate features of the denoiser ϵ_θ :

$$\text{Attention}(Q, K, V) = M \cdot V, \quad (4)$$

where $M = \text{Softmax}\left(\frac{QK^T}{\sqrt{d}}\right)$.

Query $Q = W_Q\varphi(x_t)$, key $K = W_Kc$, and value $V = W_Vc$ are computed with the learnt projections W_Q, W_K, W_V applied on intermediate spatial features $\varphi(x_t)$ of the denoising UNet ϵ_θ and the text embedding c , and d is the dimension of projected keys and queries. Of particular interest is the *cross-attention map* M , which is observed to have a tight relation with the structure of the image [22]. Individual entries of the mask $M_{i,j}$ represent the contribution of the j^{th} -th text token towards the i^{th} spatial location. Also, the cross-attention mask is specific to a timestep, and we get different attention mask M_t for each timestep t .

To apply an edit, the naive way would be to apply our pre-computed edit direction Δc_{edit} to c , and use $c_{\text{edit}} = c + \Delta c_{\text{edit}}$ for the sampling process to generate x_{edit} . This approach succeeds in changing the image according to the edit but fails to preserve the structure of the input image. As seen in the bottom row of Figure 3, the deviation of the cross-attention maps during the sampling process results in deviation in the structure of the image. As such, we propose a new *cross-attention guidance* to encourage consistency in the cross-attention maps.

We follow a two-step process, as described in Algorithm 1 and illustrated in Figure 3. First, we reconstruct the image without applying the edit direction, just using the input text c to obtain reference cross-attention maps M_t^{ref} for each timestep t . These cross-attention maps correspond to the original image’s structure e , which we aim to preserve. Next, we apply the edit direction by using c_{edit} to generate

Algorithm 1 pix2pix-zero algorithm

Input: x_T (same as x_{inv}): noise-regularized DDIM inversion of latent code corresponding to \tilde{x}
 c : input text features, Δc_{edit} : edit direction
 λ_{xa} : cross-attention guidance weight

Output: x_0 (final edited latent code)

▷ Compute reference cross-attention maps

for $t = T \dots 1$ **do**

$$\hat{e}, M_t^{\text{ref}} \leftarrow \epsilon_\theta(x_t, t, c)$$

$$x_{t-1} = \text{UPDATE}(x_t, \hat{e}, t)$$

end for

▷ Edit with cross-attention guidance

$$c_{\text{edit}} = c + \Delta c_{\text{edit}}$$

for $t = T \dots 1$ **do**

$$_, M_t^{\text{edit}} \leftarrow \epsilon_\theta(x_t, t, c_{\text{edit}})$$

$$\Delta x_t = \nabla_{x_t} (\|M_t^{\text{edit}} - M_t^{\text{ref}}\|_2)$$

$$\hat{e}, _ \leftarrow \epsilon_\theta(x_t - \lambda_{\text{xa}}\Delta x_t, t, c_{\text{edit}})$$

$$x_{t-1} = \text{UPDATE}(x_t, \hat{e}, t)$$

end for

▷ Update current state x_t with noise prediction \hat{e}

function $\text{UPDATE}(x_t, \hat{e}, t)$

$$x_{t-1} = \sqrt{\alpha_{t-1}} \frac{x_t - \sqrt{1-\alpha_t}\hat{e}}{\sqrt{\alpha_t}} + \sqrt{1-\alpha_{t-1}}\hat{e}$$

return x_{t-1}

end function

cross-attention maps M_t^{edit} . We then take a gradient step with x_t towards matching the reference M_t^{ref} , reducing the cross-attention loss \mathcal{L}_{xa} below.

$$\mathcal{L}_{\text{xa}} = \|M_t^{\text{edit}} - M_t^{\text{ref}}\|_2. \quad (5)$$

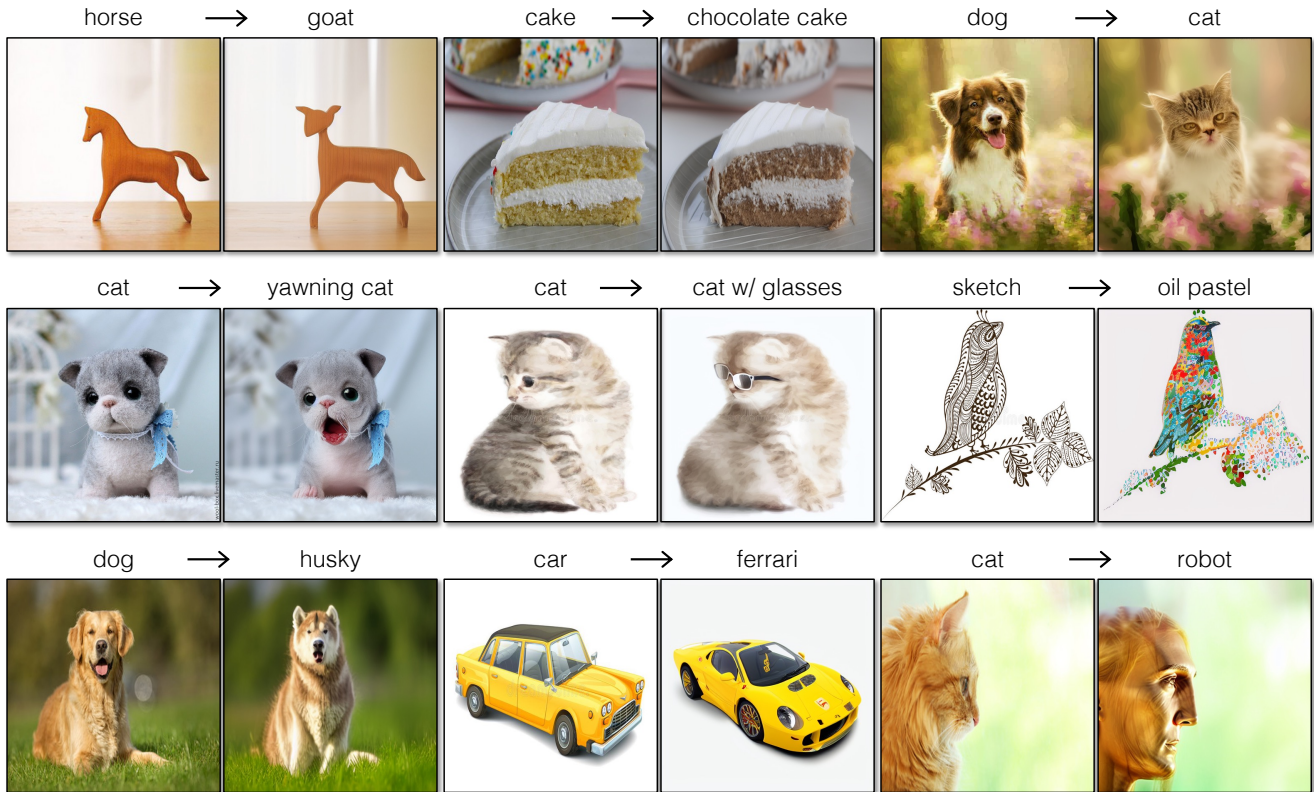
This loss encourages M_t^{edit} to not deviate from M_t^{ref} , applying the edit while retaining the original structure.

4. Experiments

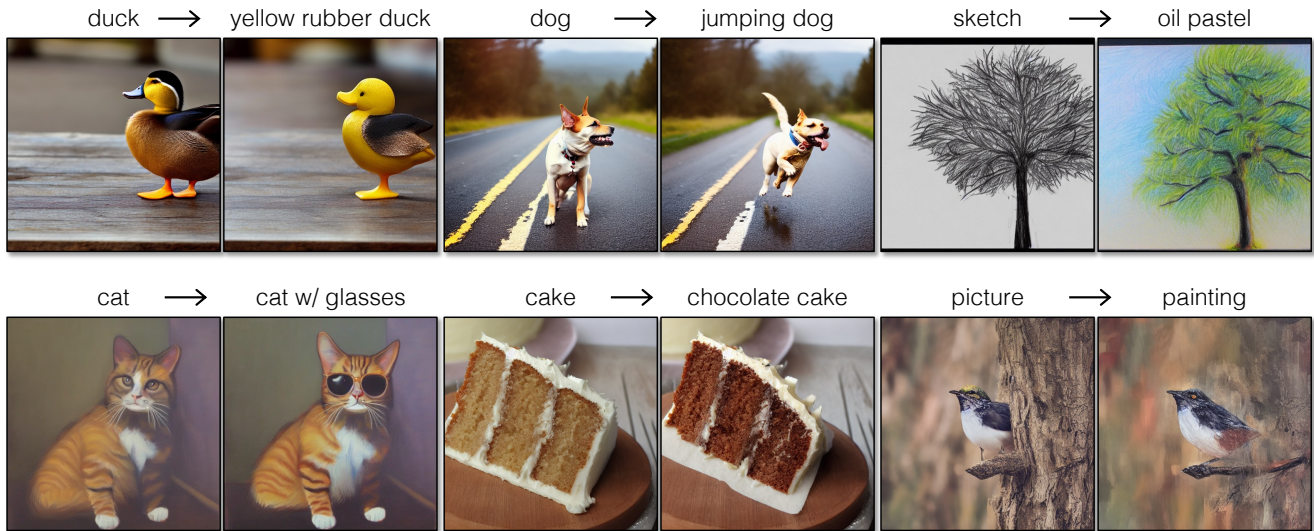
Our image-to-image translation method can be used to edit real images and control the structure of synthetic images. Next, we demonstrate our method in various experiments using Stable Diffusion v1.4 [49].

4.1. Evaluation.

Tasks. We perform quantitative evaluations using four image-to-image translation tasks: (1) translating cats to dogs (cat \rightarrow dog), (2) translating horses to zebras (horse \rightarrow zebra), (3) starting with cat input images and adding glasses (cat \rightarrow cat w/ glasses), (4) converting hand drawn sketches to oil pastel paintings (sketch \rightarrow oil pastel). All input images are taken from LAION 5B dataset. See Appendix D



real image editing



synthetic image editing

Figure 4: **Examples of pix2pix-zero results** on real (top) and synthetic images (bottom). For each image pair, we show the image before and after the edit. Note that the edit direction is generated from words alone (no prompts required). We are able to apply the edits while preserving the structure successfully.

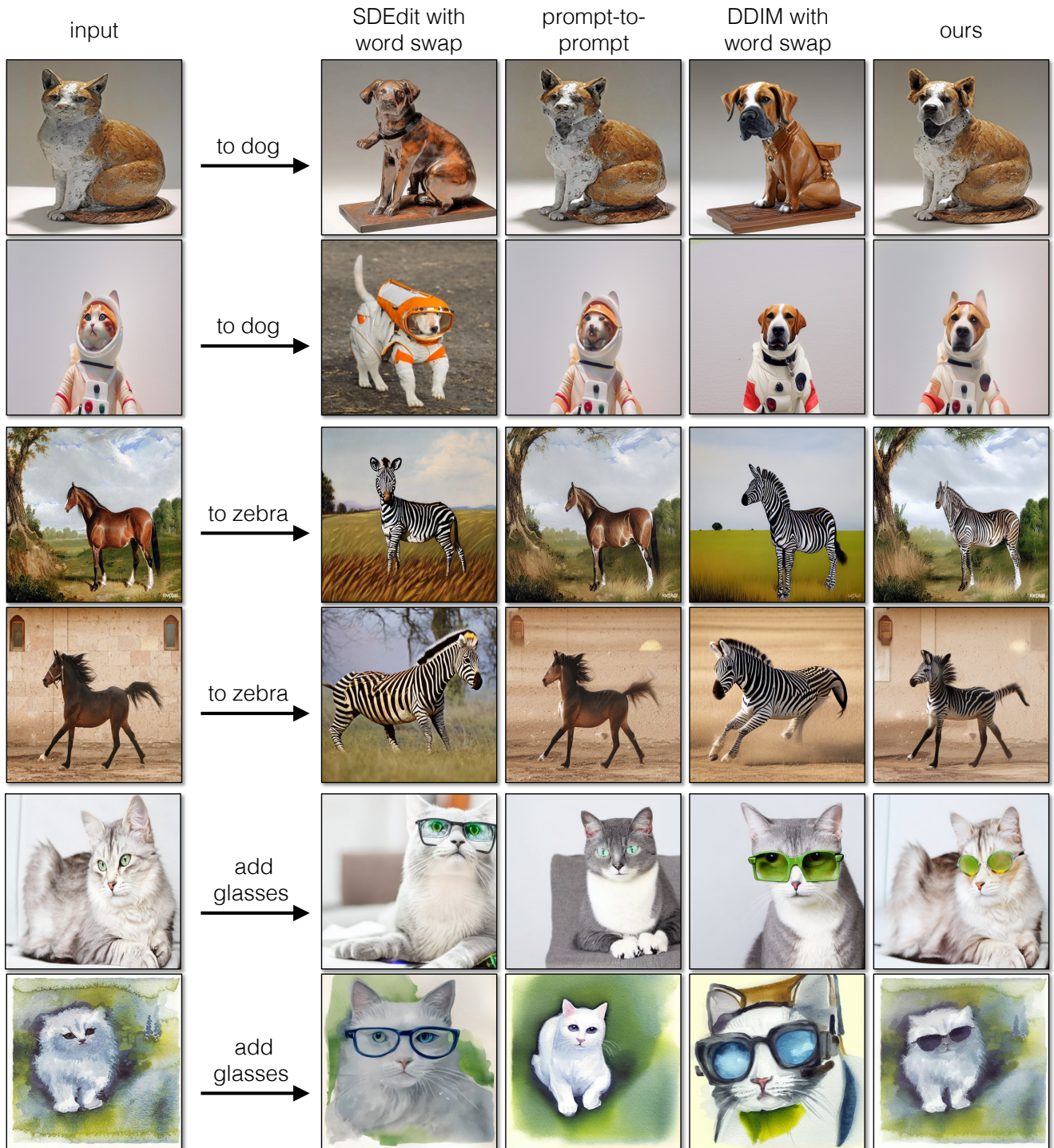


Figure 5: **Comparisons with different baselines for real images.** We observe the SDEdit [35] and DDIM [55] + word swap methods show deviation in structure, while prompt-to-prompt [22] struggles to perform the edit. Our method, as shown in the last column, successfully applies the edit, while preserving the structure of the input image.

for more details. These cover a large variety of edits, including changing the object (cat → dog, horse → zebra),

modifying the object (cat → cat w/ glasses), and changing the global style (sketch → oil pastel).

Metrics. For quantitative evaluations, we measure three criteria: (1) whether the edit was applied successfully, (2) whether the structure of the input image is retained in the edited image, and (3) if the background regions of the image stay unchanged. We measure the extent of the edit applied with CLIP Acc [23], which calculates the percentage of instances where the edited image has a higher similarity to the target text, as measured by CLIP, than to the original source text. Subsequently, the structural consistency of the edited image is measured using Structure Dist [57]. A lower score on Structure Dist means that the structure of the edited image is more similar to the input image. Lastly, to ensure that we retain the background after edits, we calculate the background LPIPS error (BG LPIPS). This is done by measuring the LPIPS distance between the background regions of the original and edited images. The background regions are identified using the object detector Detic [68]. A lower BG LPIPS score indicates that the background of the original image has been well preserved.

The background error metric BG LPIPS is only applicable for specific editing tasks where only the foreground object needs to be altered (e.g. changing a cat to a dog, or a horse to a zebra). However, for editing tasks that involve changing the entire image (e.g. converting a sketch to an oil pastel), this metric is not relevant.

4.2. Qualitative Results

In Figure 4, we show various edits applied by our approach on real (top) and synthetic images (bottom). For each result, we show pairs of images before and after editing. The edit direction is computed between the source and target, written on the top of each image pair. Our edit direction discovery method is capable of generating diverse edit directions, including changes in the type of object (e.g., from a dog to a cat or a horse to a goat), modifications of specific attributes of the object (e.g., adding sunglasses to a cat or making a cat yawn), and global style transformations of the image (e.g., from a sketch to an oil pastel or a photograph to a painting). The use of cross-attention guidance effectively preserves the structure of the original image.

4.3. Comparisons

In this section, we compare our approach to some previous and concurrent diffusion-based image editing methods. For a fair comparison, all the approaches use the Stable Diffusion [49] with the same number of sampling steps and the same classifier-free guidance for all methods. We compare against three baselines:

1) SDEdit [35] + word swap: this method first stochastically adds noise to an intermediate timestep and subsequently denoises with the new text prompt, where the source word is swapped with the target word. **2) Prompt-to-prompt [22] (concurrent work):** we use the officially re-

leased code. The method swaps the source word with the target and uses the original cross-attention map as a *hard* constraint. **3) DDIM + word swap:** we invert with the deterministic forward DDIM process and perform DDIM sampling with an edited prompt generated by swapping the source word with the target.

In Figure 5, we compare our approach with the baselines. Both the SDEdit and DDIM + word swap methods struggle to retain the structure of the input image, as they do not use the cross-attention map of the original image. Prompt-to-prompt retains the cross-attention map of the original image as a hard constraint, thus the structure. However, this comes at the cost of not performing the desired edit. In contrast, our approach utilizes the original cross-attention map as soft guidance, implemented as a loss function, allowing for flexibility in the edited cross-attention map to adapt to the chosen edit direction. As a result, we can perform the edit while preserving the structure of the input image.

In Table 1, we compare our method against the baselines and see a similar trend. SDEdit and DDIM + word swap struggle to retain the structure and the background details. On the other hand, Prompt-to-prompt gets better structure preservation and background error than SDEdit or DDIM + word swap but has a lower CLIP-Acc, indicating that the edit is applied successfully in fewer instances. Our approach gets a high CLIP-Acc while having low Structure Dist and BG LPIPS, showing we can perform the best edit while still retaining the structure and background of the original input image. We show more comparisons of synthetic images in Appendix Figure 12.

4.4. Ablation Study

Finally, we ablate each component of our method and show its effectiveness. Table 2 compares five different configurations. First, config A uses a stochastic noising process for inversion and subsequently swaps the source word with the target edit word (e.g., swapping the word “cat” with the word “dog” for the cat → dog task). Owing to the stochastic inversion, config A does not retain structure or background from the input and has a high Structure Distance and background error (BG LPIPS). Next, config B replaces the stochastic DDPM inversion with deterministic DDIM inversion and improves both the structure preservation and the background reconstruction. Config C adds the autocorrelation regularization when performing the DDIM inversion, and config D replaces the word swapping with our sentence-based edit directions. Both of these changes cause the desired edit to get applied more consistently, reflected by the improvement in CLIP Acc. Finally, config E adds the cross-attention guidance \mathcal{L}_{xa} and corresponds to our final proposed method. The cross-attention guidance helps preserve the structure of the input image and improves both the Structure Dist and BG LPIPS. Figure 6 shows this

Method	cat → dog			horse → zebra			cat → cat w/ glasses		sketch → oil pastel	
	CLIP-Acc (↑)	BG LPIPS (↓)	Structure Dist (↓)	CLIP-Acc (↑)	BG LPIPS (↓)	Structure Dist (↓)	CLIP-Acc (↑)	Structure Dist (↓)	CLIP-Acc (↑)	Structure Dist (↓)
SDEdit [35] + word swap	71.2%	0.327	0.081	92.2%	0.314	0.105	34.0%	0.082	21.2%	0.085
DDIM + word swap	72.0%	0.279	0.087	94.0%	0.283	0.123	37.6%	0.085	32.4%	0.082
prompt-to-prompt [22]	66.0%	0.269	0.080	18.4%	0.261	0.095	69.6%	0.081	10.8%	0.079
pix2pix-zero (ours)	92.4%	0.182	0.044	75.2%	0.194	0.066	71.2%	0.028	75.2%	0.052

Table 1: **Comparison to prior diffusion-based editing methods.** We compare our method to several prior diffusion-based image editing methods on four different tasks. The first two editing tasks (cat → dog, horse → zebra) are evaluated with CLIP-Acc, BG LPIPS, and Structure Dist. These metrics assess the level of editing applied, the preservation of the background, and changes in the image structure changes, respectively. The other two tasks (cat → cat w/ glasses, sketch → oil pastel) only use CLIP Acc and Structure Dist, as the background reconstruction is not relevant for these editing tasks. Our method achieves the highest CLIP classification accuracy while retaining the details from the input image, as shown through a low background LPIPS score and low structure distance.

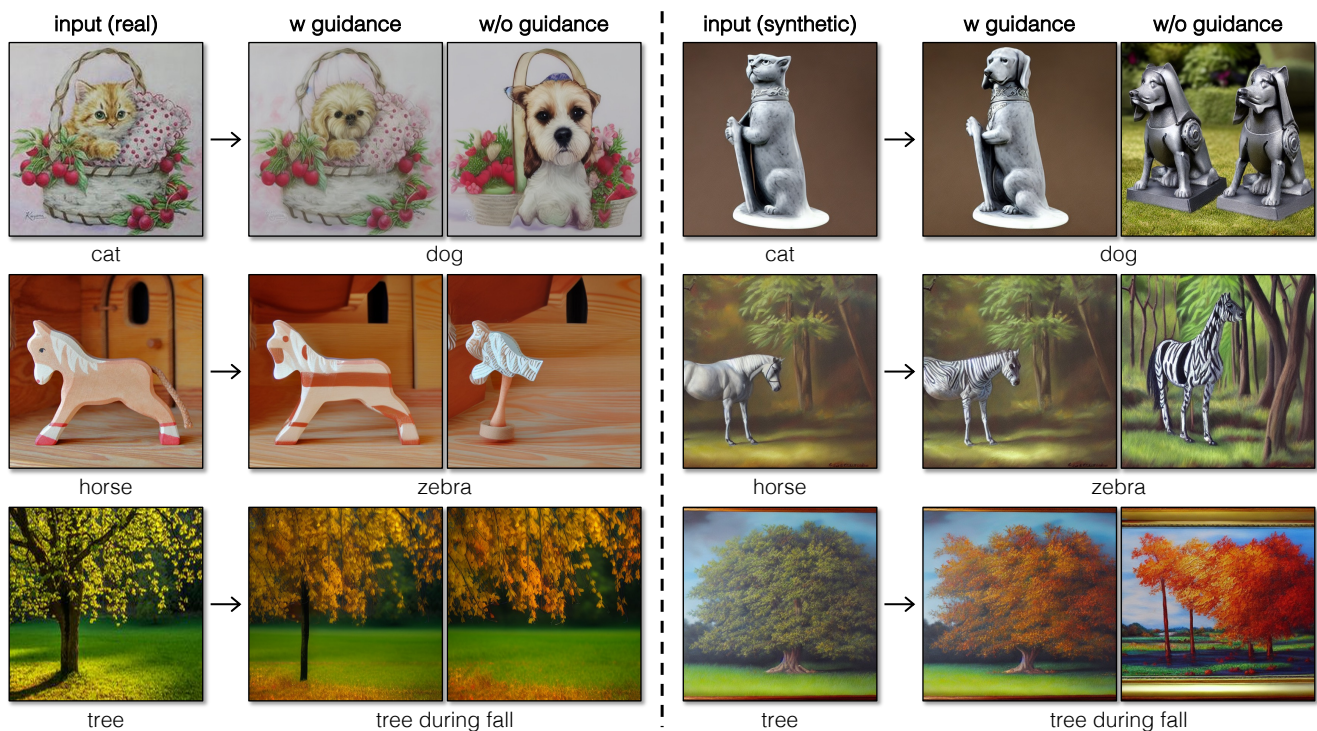


Figure 6: **Effectiveness of cross-attention guidance on structure preservation.** We show the editing results for both real (left) and synthetic (right) images. With cross-attention guidance, the structure is well-preserved for objects.

effect of cross-attention guidance qualitatively by comparing config D and config E. When cross-attention guidance is removed, the edited image does not adhere to the input image’s structure. E.g. for the task of changing cats to dogs in Figure 6, when the guidance is not used, the edited image contains a dog but in a completely different pose and different background.

4.5. Model Acceleration with Conditional GANs

One of the shortcomings of diffusion-based methods is that both inversion and sampling require many steps. To circumvent this and to train a *fast* image-to-image translation model, we can generate a *paired* dataset of input and edited images and train a paired image-conditional GAN that performs a similar edit. Figure 7 shows the results obtained by distilling using Co-Mod-GAN [67]. On a NVIDIA A100 GPU with PyTorch, the distilled model only takes 0.018

Inversion	Edit	cat → dog			horse → zebra			cat → cat w/ glasses		sketch → oil pastel		
		CLIP-Acc (↑)	BG LPIPS (↓)	Structure Dist (↓)	CLIP-Acc (↑)	BG LPIPS (↓)	Structure Dist (↓)	CLIP-Acc (↑)	Structure Dist (↓)	CLIP-Acc (↑)	Structure Dist (↓)	
A	DDPM	word swap	71.6%	0.392	0.126	93.2%	0.389	0.167	35.2%	0.122	55.2%	0.114
B	DDIM	word swap	72.0%	0.279	0.087	94.0%	0.283	0.123	37.6%	0.085	32.4%	0.082
C	DDIM w/ $\mathcal{L}_{\text{auto}}$	word swap	72.4%	0.283	0.089	94.0%	0.281	0.122	38.0%	0.087	35.2%	0.082
D	DDIM w/ $\mathcal{L}_{\text{auto}}$	sentence directions	100.0%	0.274	0.095	97.6%	0.290	0.130	20.8%	0.103	88.4%	0.087
E (ours)	DDIM w/ $\mathcal{L}_{\text{auto}}$	sentence directions w/ \mathcal{L}_{xa}	92.4%	0.182	0.044	75.2%	0.194	0.066	71.2%	0.028	75.2%	0.052

Table 2: **Ablation study.** We conduct an ablation study where we add different components of our method one at a time and observe the effects. We start with config A, which uses a naive stochastic DDPM noising process for inversion and word swap for applying the edit. This configuration does not retain the structure or the background of the input image. Config B, instead, uses deterministic DDIM inversion and results in the improvement of the structure and background preservation. Config C and D show that both regularized inversion ($\mathcal{L}_{\text{auto}}$) and sentence directions improve the editing ability. Config E, our final method, shows that using cross attention guidance \mathcal{L}_{xa} improves the background and structure preservation.

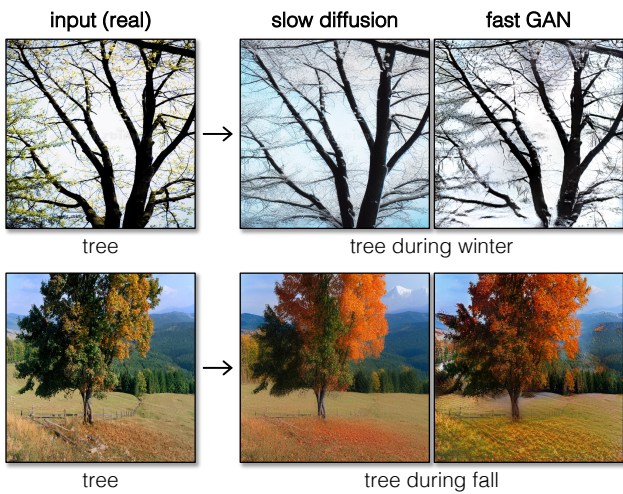


Figure 7: **Model acceleration with conditional GANs.** We show the results of the original diffusion-based model and conditional GANs for two tree editing tasks. The distilled GAN-based model achieves comparable results with a $\sim 3,800$ times speedup.

seconds per image, reducing inference time by a factor of $\sim 3,800$ times. The distilled conditional GAN can enable real-time applications, while our diffusion-based model can provide high-quality paired training data, which is expensive or impossible to collect manually.

5. Limitations and Discussion

We proposed an image-to-image translation method to perform structure-preserving image editing using a pre-trained text-to-image diffusion model. We introduced an automatic way to learn edit direction in the text embedding space. We also proposed cross-attention map guidance to preserve the structure of the original image after applying the learned edit direction. We provided detailed quantitative and qualitative results to show the effectiveness of our

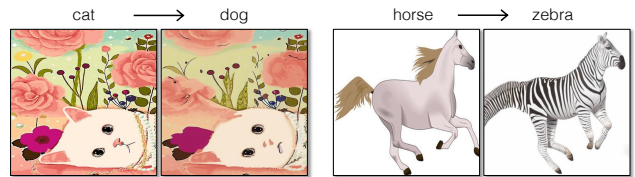


Figure 8: **Limitations.** Our method fails for difficult cases when the object pose is atypical (e.g., the cat on the left) and sometimes for preserving fine spatial position details because of the low resolution of the cross-attention maps (e.g., the leg position and the tail on the right).

approach. Our method is training-free and prompting-free.

Limitations. One of the limitations of our work is that our structure guidance is limited by the resolution of the cross-attention map. For the Stable Diffusion, the resolution for the cross-attention map is 64×64 which may not be sufficient for very fine-grained structure control (as shown in Figure 8, our edited zebra does not follow fine-grained details of leg and tail). Although our approach can work with any resolution of cross-attention map, if the base model has a higher resolution for cross-attention map, then our approach can provide even finer structure guidance control. Also, the method can fail in difficult cases of objects having atypical poses (cat in Figure 8).

Acknowledgments. This work was partly done by Gaurav Parmar during the Adobe internship. We thank Sheng-Yu Wang, Gautam Gare, Nupur Kumari, Muyang Li, Ruihan Gao, Aniruddha Mahapatra, and Yotam Nitzan for proofreading our manuscript and feedback. We are also grateful to Kangle Deng, George Cazenavette, Chonghyuk (Andrew) Song, Alyosha Efros, and Phillip Isola for fruitful discussions. This project is partly supported by Adobe Inc.

References

- [1] Rameen Abdal, Yipeng Qin, and Peter Wonka. Image2stylegan: How to embed images into the stylegan latent space? In *IEEE International Conference on Computer Vision (ICCV)*, 2019. 2
- [2] Rameen Abdal, Yipeng Qin, and Peter Wonka. Image2stylegan++: How to edit the embedded images? In *IEEE Conference on Computer Vision and Pattern Recognition (CVPR)*, 2020. 2
- [3] Rameen Abdal, Peihao Zhu, John Femiani, Niloy Mitra, and Peter Wonka. Clip2stylegan: Unsupervised extraction of stylegan edit directions. In *ACM SIGGRAPH 2022 Conference Proceedings*, SIGGRAPH '22, New York, NY, USA, 2022. Association for Computing Machinery. 2
- [4] Omri Avrahami, Dani Lischinski, and Ohad Fried. Blended diffusion for text-driven editing of natural images. In *Proceedings of the IEEE/CVF Conference on Computer Vision and Pattern Recognition*, pages 18208–18218, 2022. 3
- [5] Kyungjune Baek, Yunjey Choi, Youngjung Uh, Jaejun Yoo, and Hyunjun Shim. Rethinking the truly unsupervised image-to-image translation. In *Proceedings of the IEEE/CVF International Conference on Computer Vision*, pages 14154–14163, 2021. 2
- [6] Dzmitry Bahdanau, Kyunghyun Cho, and Yoshua Bengio. Neural machine translation by jointly learning to align and translate. *arXiv preprint arXiv:1409.0473*, 2014. 5
- [7] David Bau, Alex Andonian, Audrey Cui, YeonHwan Park, Ali Jahanian, Aude Oliva, and Antonio Torralba. Paint by word. *arXiv preprint arXiv:2103.10951*, 2021. 2
- [8] David Bau, Hendrik Strobelt, William Peebles, Jonas Wulff, Bolei Zhou, Jun-Yan Zhu, and Antonio Torralba. Semantic photo manipulation with a generative image prior. *ACM Transactions on Graphics (TOG)*, 38(4):1–11, 2019. 2
- [9] Romain Beaumont. clip-retrieval. <https://github.com/rom1504/clip-retrieval>, 2022. 14
- [10] Tim Brooks, Aleksander Holynski, and Alexei A Efros. Instructpix2pix: Learning to follow image editing instructions. *arXiv preprint arXiv:2211.09800*, 2022. 3
- [11] Tom Brown, Benjamin Mann, Nick Ryder, Melanie Subbiah, Jared D Kaplan, Prafulla Dhariwal, Arvind Neelakantan, Pranav Shyam, Girish Sastry, Amanda Askell, et al. Language models are few-shot learners. *Advances in neural information processing systems*, 33:1877–1901, 2020. 4
- [12] Lucy Chai, David Bau, Ser-Nam Lim, and Phillip Isola. What makes fake images detectable? understanding properties that generalize. In *Computer Vision—ECCV 2020: 16th European Conference, Glasgow, UK, August 23–28, 2020, Proceedings, Part XXVI 16*, pages 103–120. Springer, 2020. 15, 16
- [13] Jooyoung Choi, Sungwon Kim, Yonghyun Jeong, Youngjune Gwon, and Sungroh Yoon. Ilvr: Conditioning method for denoising diffusion probabilistic models. *arXiv preprint arXiv:2108.02938*, 2021. 3
- [14] Yunjey Choi, Minje Choi, Munyoung Kim, Jung-Woo Ha, Sunghun Kim, and Jaegul Choo. Stargan: Unified generative adversarial networks for multi-domain image-to-image translation. In *IEEE Conference on Computer Vision and Pattern Recognition (CVPR)*, 2018. 2
- [15] Riccardo Corvi, Davide Cozzolino, Giada Zingarini, Giovanni Poggi, Koki Nagano, and Luisa Verdoliva. On the detection of synthetic images generated by diffusion models. *arXiv preprint arXiv:2211.00680*, 2022. 15
- [16] Prafulla Dhariwal and Alexander Nichol. Diffusion models beat gans on image synthesis. In *Conference on Neural Information Processing Systems (NeurIPS)*, 2021. 14
- [17] Ming Ding, Zhuoyi Yang, Wenyi Hong, Wendi Zheng, Chang Zhou, Da Yin, Junyang Lin, Xu Zou, Zhou Shao, Hongxia Yang, et al. Cogview: Mastering text-to-image generation via transformers. *Advances in Neural Information Processing Systems*, 34:19822–19835, 2021. 3
- [18] Oran Gafni, Adam Polyak, Oron Ashual, Shelly Sheynin, Devi Parikh, and Yaniv Taigman. Make-a-scene: Scene-based text-to-image generation with human priors. *arXiv preprint arXiv:2203.13131*, 2022. 3
- [19] Jinjin Gu, Yujun Shen, and Bolei Zhou. Image processing using multi-code gan prior. In *IEEE Conference on Computer Vision and Pattern Recognition (CVPR)*, 2020. 2
- [20] John A Gubner. *Probability and random processes for electrical and computer engineers*. Cambridge University Press, 2006. 4
- [21] Erik Härkönen, Aaron Hertzmann, Jaakko Lehtinen, and Sylvain Paris. Ganspace: Discovering interpretable gan controls. In *Neural Information Processing Systems (NeurIPS)*, 2020. 2
- [22] Amir Hertz, Ron Mokady, Jay Tenenbaum, Kfir Aberman, Yael Pritch, and Daniel Cohen-Or. Prompt-to-prompt image editing with cross attention control. *arXiv preprint arXiv:2208.01626*, 2022. 2, 3, 5, 7, 8, 9, 14, 17
- [23] Jack Hessel, Ari Holtzman, Maxwell Forbes, Ronan Le Bras, and Yejin Choi. CLIPScore: a reference-free evaluation metric for image captioning. In *EMNLP*, 2021. 8
- [24] Jonathan Ho, Ajay Jain, and Pieter Abbeel. Denoising diffusion probabilistic models. In *Neural Information Processing Systems (NeurIPS)*, 2020. 3
- [25] Jonathan Ho and Tim Salimans. Classifier-free diffusion guidance. *arXiv preprint arXiv:2207.12598*, 2022. 15
- [26] Xun Huang, Ming-Yu Liu, Serge Belongie, and Jan Kautz. Multimodal unsupervised image-to-image translation. *European Conference on Computer Vision (ECCV)*, 2018. 2
- [27] Minyoung Huh, Richard Zhang, Jun-Yan Zhu, Sylvain Paris, and Aaron Hertzmann. Transforming and projecting images into class-conditional generative networks. In *European Conference on Computer Vision (ECCV)*, 2020. 2
- [28] Phillip Isola, Jun-Yan Zhu, Tinghui Zhou, and Alexei A Efros. Image-to-image translation with conditional adversarial networks. In *IEEE Conference on Computer Vision and Pattern Recognition (CVPR)*, 2017. 2
- [29] Tero Karras, Samuli Laine, Miika Aittala, Janne Hellsten, Jaakko Lehtinen, and Timo Aila. Analyzing and improving the image quality of stylegan. In *IEEE Conference on Computer Vision and Pattern Recognition (CVPR)*, 2020. 4
- [30] Bahjat Kawar, Shiran Zada, Oran Lang, Omer Tov, Huiwen Chang, Tali Dekel, Inbar Mosseri, and Michal Irani. Imagic:

- Text-based real image editing with diffusion models. *arXiv preprint arXiv:2210.09276*, 2022. 3
- [31] Gwanghyun Kim, Taesung Kwon, and Jong Chul Ye. Diffusionclip: Text-guided diffusion models for robust image manipulation. In *IEEE Conference on Computer Vision and Pattern Recognition (CVPR)*, 2022. 14
- [32] Diederik P Kingma and Max Welling. Auto-encoding variational bayes. In *International Conference on Learning Representations (ICLR)*, 2014. 4
- [33] Junnan Li, Dongxu Li, Caiming Xiong, and Steven Hoi. Blip: Bootstrapping language-image pre-training for unified vision-language understanding and generation. In *International Conference on Machine Learning (ICML)*, 2022. 3, 4
- [34] Ming-Yu Liu, Thomas Breuel, and Jan Kautz. Unsupervised image-to-image translation networks. In *Neural Information Processing Systems (NeurIPS)*, 2017. 2
- [35] Chenlin Meng, Yang Song, Jiaming Song, Jiajun Wu, Jun-Yan Zhu, and Stefano Ermon. Sdedit: Image synthesis and editing with stochastic differential equations. *arXiv preprint arXiv:2108.01073*, 2021. 2, 3, 7, 8, 9, 14, 17
- [36] Lakshmanan Nataraj, Tajuddin Manhar Mohammed, BS Manjunath, Shivkumar Chandrasekaran, Arjuna Flenner, Jawadul H Bappy, and Amit K Roy-Chowdhury. Detecting gan generated fake images using co-occurrence matrices. *Electronic Imaging*, 2019. 15
- [37] Alex Nichol, Prafulla Dhariwal, Aditya Ramesh, Pranav Shyam, Pamela Mishkin, Bob McGrew, Ilya Sutskever, and Mark Chen. Glide: Towards photorealistic image generation and editing with text-guided diffusion models. *arXiv preprint arXiv:2112.10741*, 2021. 3
- [38] Xingang Pan, Xiaohang Zhan, Bo Dai, Dahua Lin, Chen Change Loy, and Ping Luo. Exploiting deep generative prior for versatile image restoration and manipulation. *IEEE Transactions on Pattern Analysis and Machine Intelligence (TPAMI)*, 2021. 2
- [39] Taesung Park, Ming-Yu Liu, Ting-Chun Wang, and Jun-Yan Zhu. Semantic image synthesis with spatially-adaptive normalization. In *IEEE Conference on Computer Vision and Pattern Recognition (CVPR)*, 2019. 2
- [40] Gaurav Parmar, Yijun Li, Jingwan Lu, Richard Zhang, Jun-Yan Zhu, and Krishna Kumar Sing. Spatially-adaptive multi-layer selection for gan inversion and editing. In *Proceedings of the IEEE/CVF Conference on Computer Vision and Pattern Recognition*, 2022. 2
- [41] Or Patashnik, Zongze Wu, Eli Shechtman, Daniel Cohen-Or, and Dani Lischinski. Styleclip: Text-driven manipulation of stylegan imagery. In *Proceedings of the IEEE/CVF International Conference on Computer Vision (ICCV)*, 2021. 2
- [42] Alec Radford, Jong Wook Kim, Chris Hallacy, Aditya Ramesh, Gabriel Goh, Sandhini Agarwal, Girish Sastry, Amanda Askell, Pamela Mishkin, Jack Clark, et al. Learning transferable visual models from natural language supervision. In *International Conference on Machine Learning*, pages 8748–8763. PMLR, 2021. 5
- [43] Aditya Ramesh, Prafulla Dhariwal, Alex Nichol, Casey Chu, and Mark Chen. Hierarchical text-conditional image generation with clip latents. *arXiv preprint arXiv:2204.06125*, 2022. 2, 3, 5
- [44] Aditya Ramesh, Mikhail Pavlov, Gabriel Goh, Scott Gray, Chelsea Voss, Alec Radford, Mark Chen, and Ilya Sutskever. Zero-shot text-to-image generation. *arXiv preprint arXiv:2102.12092*, 2021. 3
- [45] Elad Richardson, Yuval Alaluf, Or Patashnik, Yotam Nitzan, Yaniv Azar, Stav Shapiro, and Daniel Cohen-Or. Encoding in style: a stylegan encoder for image-to-image translation. *arXiv preprint arXiv:2008.00951*, 2020. 2
- [46] Daniel Roich, Ron Mokady, Amit H Bermano, and Daniel Cohen-Or. Pivotal tuning for latent-based editing of real images. *arXiv preprint arXiv:2106.05744*, 2021. 2
- [47] Robin Rombach, Andreas Blattmann, Dominik Lorenz, Patrick Esser, and Björn Ommer. High-resolution image synthesis with latent diffusion models. In *Proceedings of the IEEE/CVF Conference on Computer Vision and Pattern Recognition*, pages 10684–10695, 2022. 2, 3, 5
- [48] Robin Rombach, Andreas Blattmann, Dominik Lorenz, Patrick Esser, and Björn Ommer. High-resolution image synthesis with latent diffusion models. In *IEEE Conference on Computer Vision and Pattern Recognition (CVPR)*, 2022. 5
- [49] Robin Rombach, Andreas Blattmann, Dominik Lorenz, Patrick Esser, and Björn Ommer. Stable Diffusion. <https://github.com/CompVis/stable-diffusion>, 2022. 5, 8
- [50] Chitwan Saharia, William Chan, Huiwen Chang, Chris Lee, Jonathan Ho, Tim Salimans, David Fleet, and Mohammad Norouzi. Palette: Image-to-image diffusion models. In *ACM SIGGRAPH*, pages 1–10, 2022. 3
- [51] Chitwan Saharia, William Chan, Saurabh Saxena, Lala Li, Jay Whang, Emily Denton, Seyed Kamyar Seyed Ghasemipour, Burcu Karagol Ayan, S Sara Mahdavi, Rapha Gontijo Lopes, et al. Photorealistic text-to-image diffusion models with deep language understanding. *arXiv preprint arXiv:2205.11487*, 2022. 2, 3, 5
- [52] Patsorn Sangkloy, Jingwan Lu, Chen Fang, Fisher Yu, and James Hays. Scribbler: Controlling deep image synthesis with sketch and color. In *IEEE Conference on Computer Vision and Pattern Recognition (CVPR)*, 2017. 2
- [53] Zeyang Sha, Zheng Li, Ning Yu, and Yang Zhang. De-fake: Detection and attribution of fake images generated by text-to-image diffusion models. *arXiv preprint arXiv:2210.06998*, 2022. 15
- [54] Yujun Shen, Ceyuan Yang, Xiaou Tang, and Bolei Zhou. Interfacegan: Interpreting the disentangled face representation learned by gans. *IEEE Transactions on Pattern Analysis and Machine Intelligence (TPAMI)*, 2020. 2
- [55] Jiaming Song, Chenlin Meng, and Stefano Ermon. Denoising diffusion implicit models. In *International Conference on Learning Representations (ICLR)*, 2021. 2, 3, 7, 14, 17
- [56] Yang Song, Jascha Sohl-Dickstein, Diederik P Kingma, Abhishek Kumar, Stefano Ermon, and Ben Poole. Score-based generative modeling through stochastic differential equations. *arXiv preprint arXiv:2011.13456*, 2020. 3
- [57] Narek Tumanyan, Omer Bar-Tal, Shai Bagon, and Tali Dekel. Splicing vit features for semantic appearance transfer.

- In *Proceedings of the IEEE/CVF Conference on Computer Vision and Pattern Recognition*, pages 10748–10757, 2022. 8
- [58] Ashish Vaswani, Noam Shazeer, Niki Parmar, Jakob Uszkoreit, Llion Jones, Aidan N Gomez, Łukasz Kaiser, and Illia Polosukhin. Attention is all you need. In *Conference on Neural Information Processing Systems (NeurIPS)*, 2017. 5
- [59] Sheng-Yu Wang, Oliver Wang, Richard Zhang, Andrew Owens, and Alexei A Efros. Cnn-generated images are surprisingly easy to spot...for now. In *IEEE Conference on Computer Vision and Pattern Recognition (CVPR)*, 2020. 15, 16
- [60] Tengfei Wang, Ting Zhang, Bo Zhang, Hao Ouyang, Dong Chen, Qifeng Chen, and Fang Wen. Pretraining is all you need for image-to-image translation. *arXiv preprint arXiv:2205.12952*, 2022. 3
- [61] Ting-Chun Wang, Ming-Yu Liu, Jun-Yan Zhu, Andrew Tao, Jan Kautz, and Bryan Catanzaro. High-resolution image synthesis and semantic manipulation with conditional gans. In *IEEE Conference on Computer Vision and Pattern Recognition (CVPR)*, 2018. 2
- [62] Zongze Wu, Dani Lischinski, and Eli Shechtman. Stylespace analysis: Disentangled controls for stylegan image generation. In *IEEE Conference on Computer Vision and Pattern Recognition (CVPR)*, 2021. 2
- [63] Jonas Wulff and Antonio Torralba. Improving inversion and generation diversity in stylegan using a gaussianized latent space. *arXiv preprint arXiv:2009.06529*, 2020. 2
- [64] Jiahui Yu, Yuanzhong Xu, Jing Yu Koh, Thang Luong, Gungjan Baid, Zirui Wang, Vijay Vasudevan, Alexander Ku, Yinfei Yang, Burcu Karagol Ayan, et al. Scaling autoregressive models for content-rich text-to-image generation. *arXiv preprint arXiv:2206.10789*, 2022. 3
- [65] Ning Yu, Larry S Davis, and Mario Fritz. Attributing fake images to gans: Learning and analyzing gan fingerprints. In *Proceedings of the IEEE/CVF international conference on computer vision*, pages 7556–7566, 2019. 15
- [66] Richard Zhang, Phillip Isola, Alexei A Efros, Eli Shechtman, and Oliver Wang. The unreasonable effectiveness of deep features as a perceptual metric. In *IEEE Conference on Computer Vision and Pattern Recognition (CVPR)*, 2018. 14
- [67] Shengyu Zhao, Jonathan Cui, Yilun Sheng, Yue Dong, Xiao Liang, Eric I Chang, and Yan Xu. Large scale image completion via co-modulated generative adversarial networks. In *International Conference on Learning Representations (ICLR)*, 2021. 9, 14
- [68] Xingyi Zhou, Rohit Girdhar, Armand Joulin, Philipp Krähenbühl, and Ishan Misra. Detecting twenty-thousand classes using image-level supervision. In *European Conference on Computer Vision (ECCV)*, 2022. 8
- [69] Jiapeng Zhu, Yujun Shen, Deli Zhao, and Bolei Zhou. In-domain gan inversion for real image editing. In *European Conference on Computer Vision (ECCV)*, 2020. 2
- [70] Jun-Yan Zhu, Philipp Krähenbühl, Eli Shechtman, and Alexei A Efros. Generative visual manipulation on the natural image manifold. In *European Conference on Computer Vision (ECCV)*, 2016. 2
- [71] Jun-Yan Zhu, Taesung Park, Phillip Isola, and Alexei A Efros. Unpaired image-to-image translation using cycle-consistent adversarial networks. In *IEEE International Conference on Computer Vision (ICCV)*, 2017. 2

Appendix

We start with Appendix A, which shows additional details about how the fast distilled GAN-based model is trained and provides additional results. Next, in Appendix B and Appendix C, we show some more comparisons with baselines and the effects of regularization, respectively. Appendix D provides the experiment details. Finally, in Appendix E, we discuss some of the societal impacts of this line of research. We show additional qualitative results in Figures 13, 14, 15, and 16.

A. Fast Distillation

Section 4.5 of the main paper discusses distilling a slow, text-to-image diffusion model into a fast, feed-forward model. Here, we describe additional implementation details.

Paired Dataset Collection. We first collect 15,000 pairs of input and edited images generated by our editing method proposed in the main paper. Next, we automatically filter out pairs with low segmentation overlap or do not sufficiently increase the CLIP similarity with the target description. For the cat to dog task, we use a segmentation threshold of 0.70 and a CLIP increase threshold of 0.10. For the tree to winter trees and fall trees tasks, we only use a CLIP increase threshold of 0.1 as the off-the-shelf segmentation model does not reliably segment trees in the image.

Fast GAN Training. Given pairs of input and edited images, we train a CoModGAN [67] to perform image translation. For all experiments, we use a learning rate of 0.001 and a batch size of 64. Additionally, we apply data augmentation in the form of standard color transformations (brightness, contrast, hue, saturation), adding noise, and random crops. We optimize a reconstruction objective using a combination of L1 distance and VGG-based LPIPS [66].

More Results. In Figure 10 and Figure 11, we show the results of our fast distilled GAN model for the tree to winter tree and fall tree tasks, respectively. Our fast GAN model gives comparable results regarding edit quality and structure perseverance at a much faster inference speed.

B. Comparisons to Baselines.

Figure 5 and Section 4.3 in the main paper compare the image editing performance of various methods on *real* images. In Figure 12, we show a similar comparison of synthetic image editing. Our observations are consistent with the real images shown in the main paper. Our method is able to respect the structure of the input image while performing the requested edit. SDEdit [35] and DDIM [55]

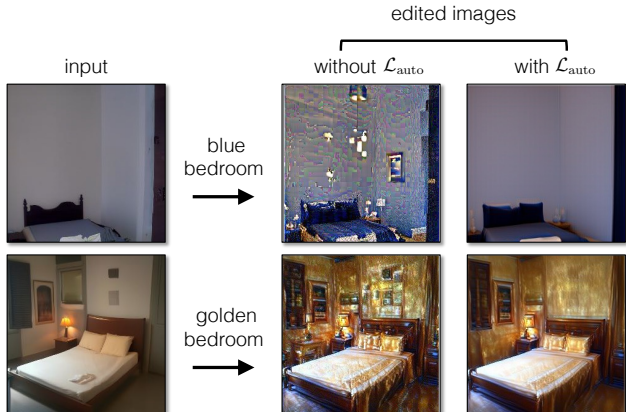


Figure 9: **Qualitative effects of regularization on smaller models.** Here, we show editing results using Diffusion-CLIP with and without our regularization. We can see that our regularization is critical for reducing the artifact in the edited results.

with word swap struggle to preserve the structure. prompt-to-prompt [22] works better on synthetic images compared to real images but still struggles to achieve desired edits in some cases (e.g. zebra stripes are not applied correctly).

C. Ablations

Effects of Regularization during Inversion. In Table 2 of the main paper, we show the importance of our regularization $\mathcal{L}_{\text{auto}}$, which was introduced in Section 3.1 of the main paper. Using this regularization helps improve the extent of editing applied, as indicated by a better CLIP Acc score. Our regularization encourages the inverted noise to be more Gaussian, which makes our edit direction more compatible and less inclined to make undesired structure changes. We also observe that the effects of the regularization are more pronounced when using smaller-scale diffusion models trained for specific categories. In Figure 9, we show image editing results using a smaller diffusion model [16] trained on the LSUN Bedrooms and finetuned following DiffusionCLIP [31] to perform the edit. Inverting without regularization and subsequently editing results in noticeable artifacts.

D. Experiment Details

Dataset. We use subsets of the LAION 5B dataset for all real image editing experiments. We retrieve 250 relevant images from the dataset by matching CLIP embeddings of the source text description and applying an aesthetics filter of 9 [9]. For example, in the cat \rightarrow dog translation, we retrieve images from the dataset with a high CLIP similarity with the source word cat.

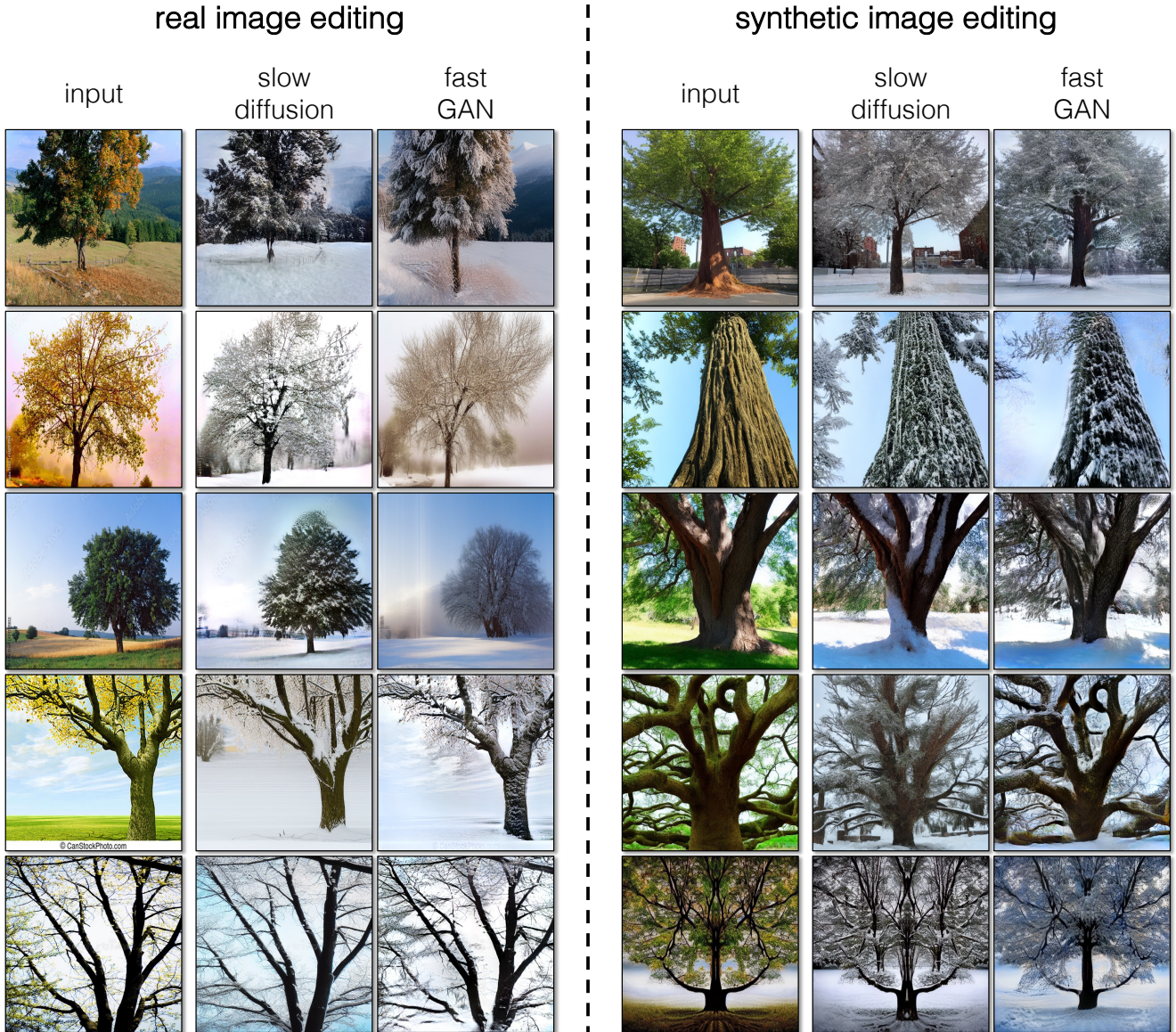


Figure 10: **Model acceleration with conditional GANs.** Here, we show fast GAN distillation and the slower diffusion editing results for the task of tree \rightarrow tree during winter. Our distilled conditional GAN achieves comparable results regarding image quality and structure preservation at a significantly reduced cost.

Baselines. For all results shown in Figure 5, Table 1 in the main paper, and Figure 12, we use the official code released by the authors and follow the recommended hyper-parameters.

Implementation Details. For all results shown for our method, we use 100 steps for DDIM inversion and 100 steps for both reconstruction and editing. During DDIM inversion, we apply the noise regularization for 5 iterations at each timestep and use a weight λ of 20. Additionally, we use classifier-free guidance [25] for all editing results.

E. Societal Impact

Our work is part of a broader movement toward democratizing content creation with generative models. We aim to allow users to create new content with precise control over the desired edit. Even though the primary usage of our work is in the creative industry, it can be potentially used to fabricate images for malicious practices. However, a line of work has studied whether generated images are detectable, in the context of GANs [65, 36, 12, 59] and more recently, diffusion models [15, 53]. Such work

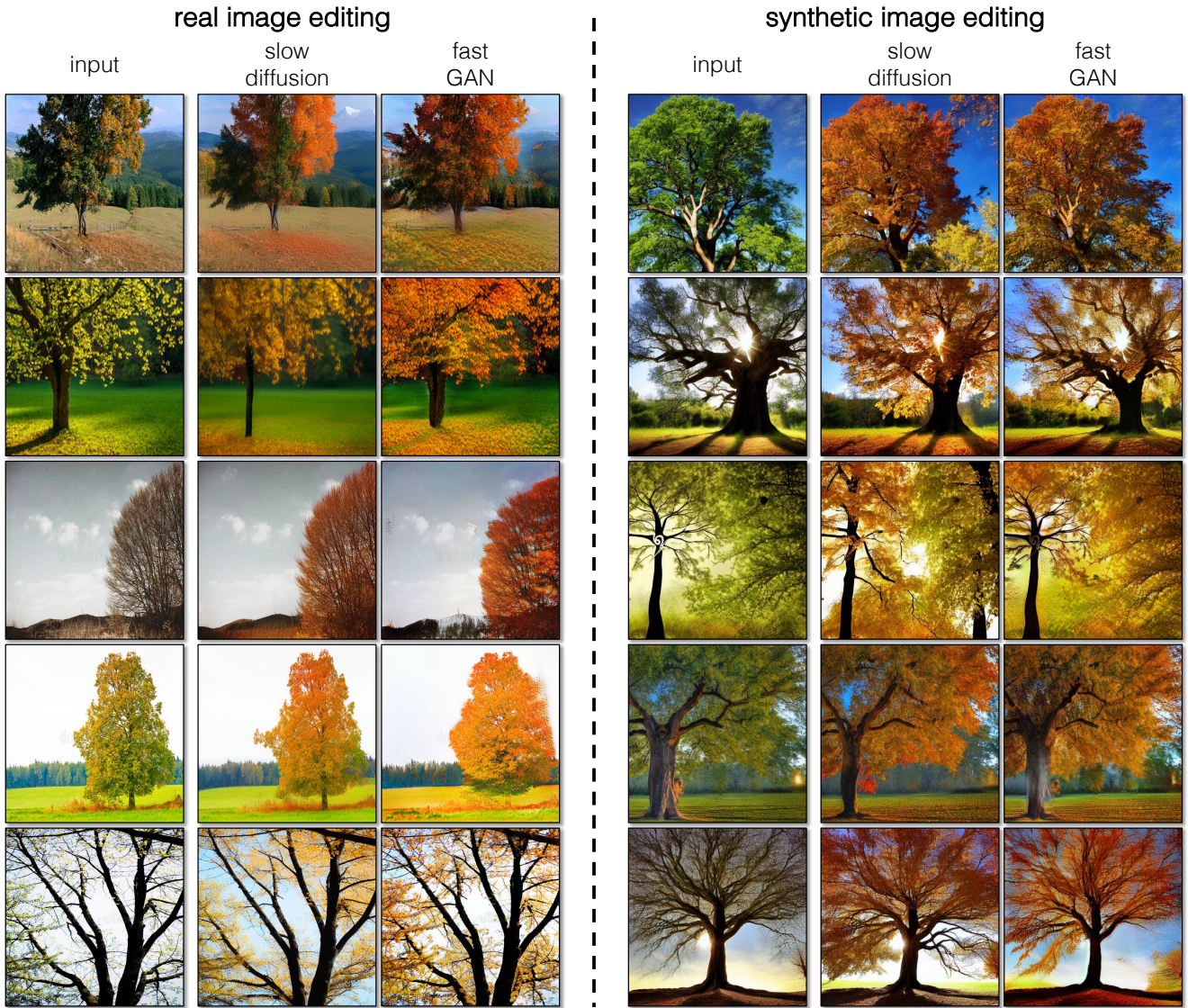


Figure 11: **Model acceleration with conditional GANs.** Here, we show the fast GAN distillation and the slower diffusion editing results for the task of tree \rightarrow tree during fall. Our distilled conditional GAN achieves comparable results regarding image quality and structure preservation at a significantly reduced cost.

has suggested that while generators produce realistic images, they can still generate consistently detectable artifacts across methods [12, 59], enabling their downstream identification.

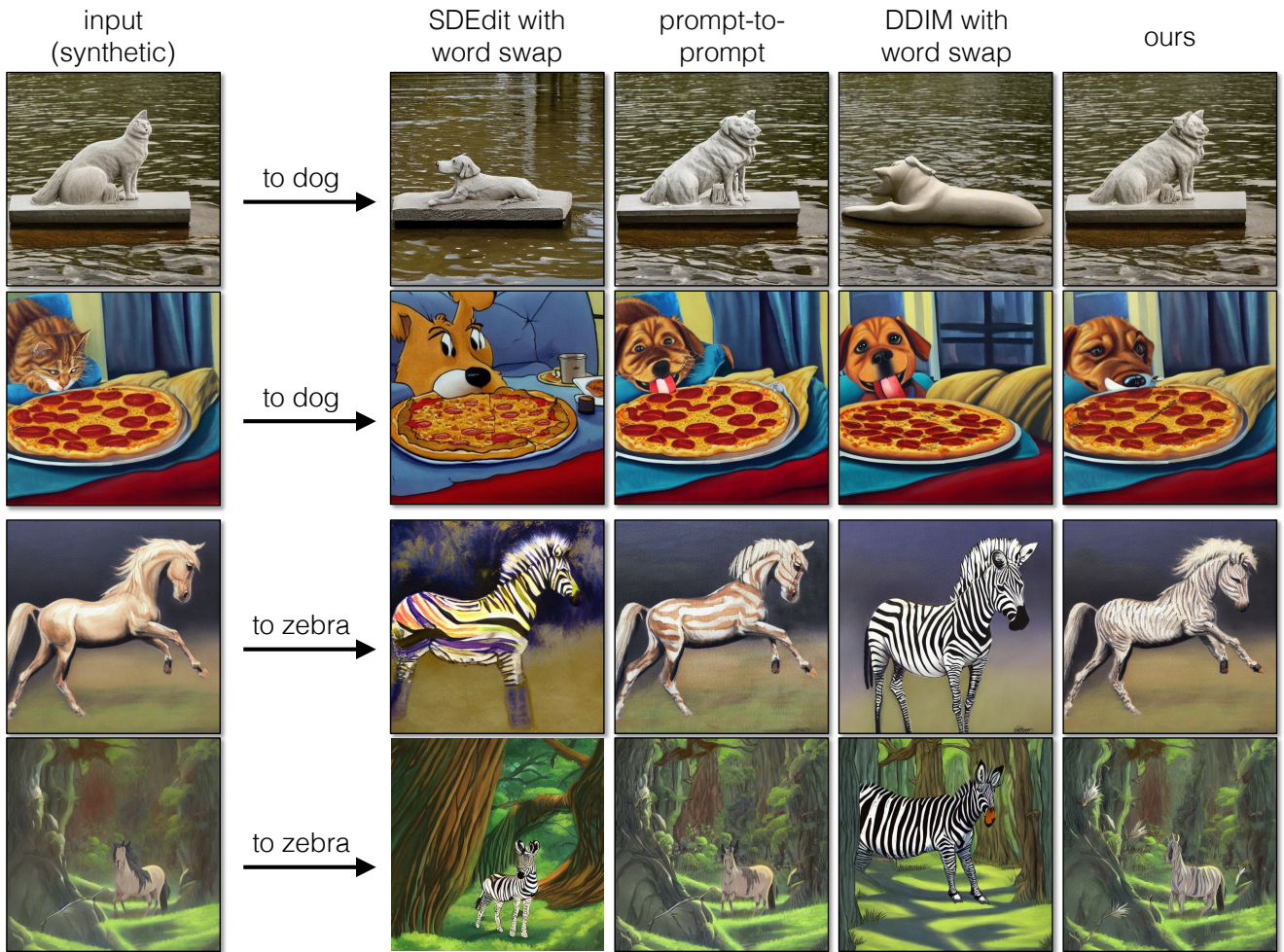


Figure 12: **Comparing to baseline approaches.** We compare our approach with baselines on synthetic images. Our approach does a better job of preserving the structure while performing edits compared to SDEdit [35] and DDIM [55] with word swap. prompt-to-prompt [22] succeeds to preserve the structure but with lower editing quality.

real image editing (cat → dog)

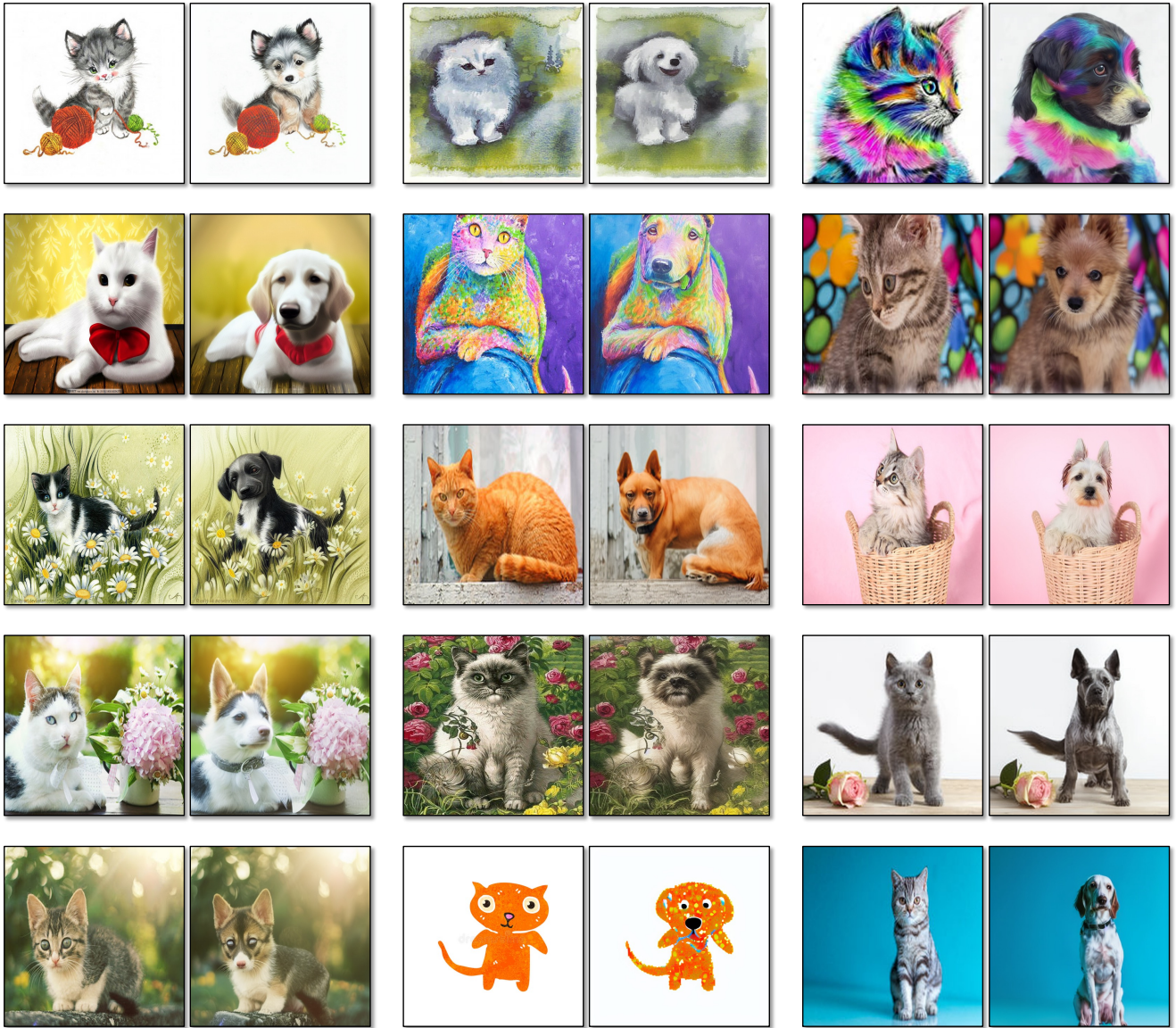


Figure 13: **Additional results.** We show additional results on real images for the cat → dog task.

real image editing (dog \rightarrow cat)

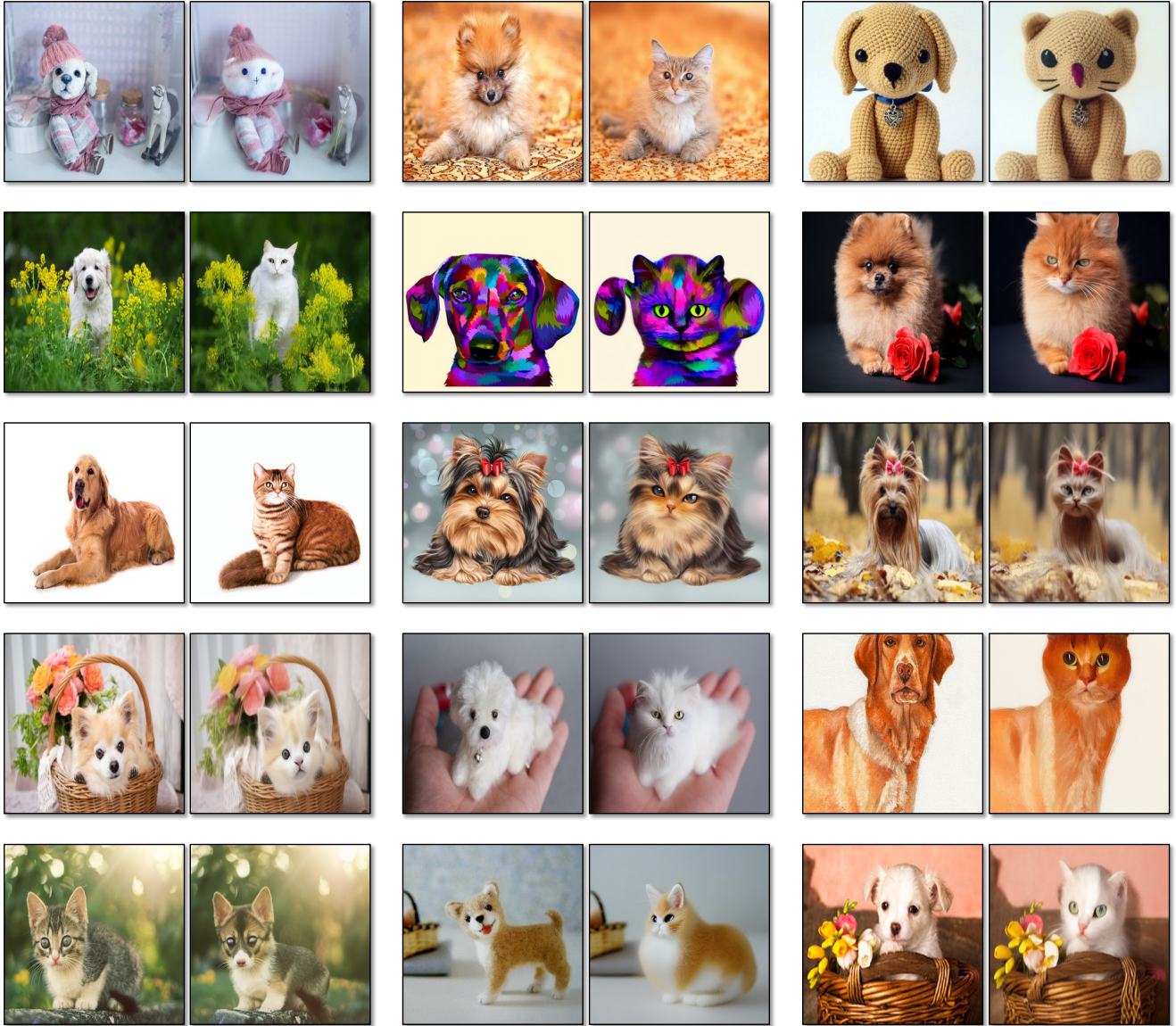


Figure 14: **Additional results.** We show additional results on real images for the dog \rightarrow cat task.

real image editing (horse → zebra)

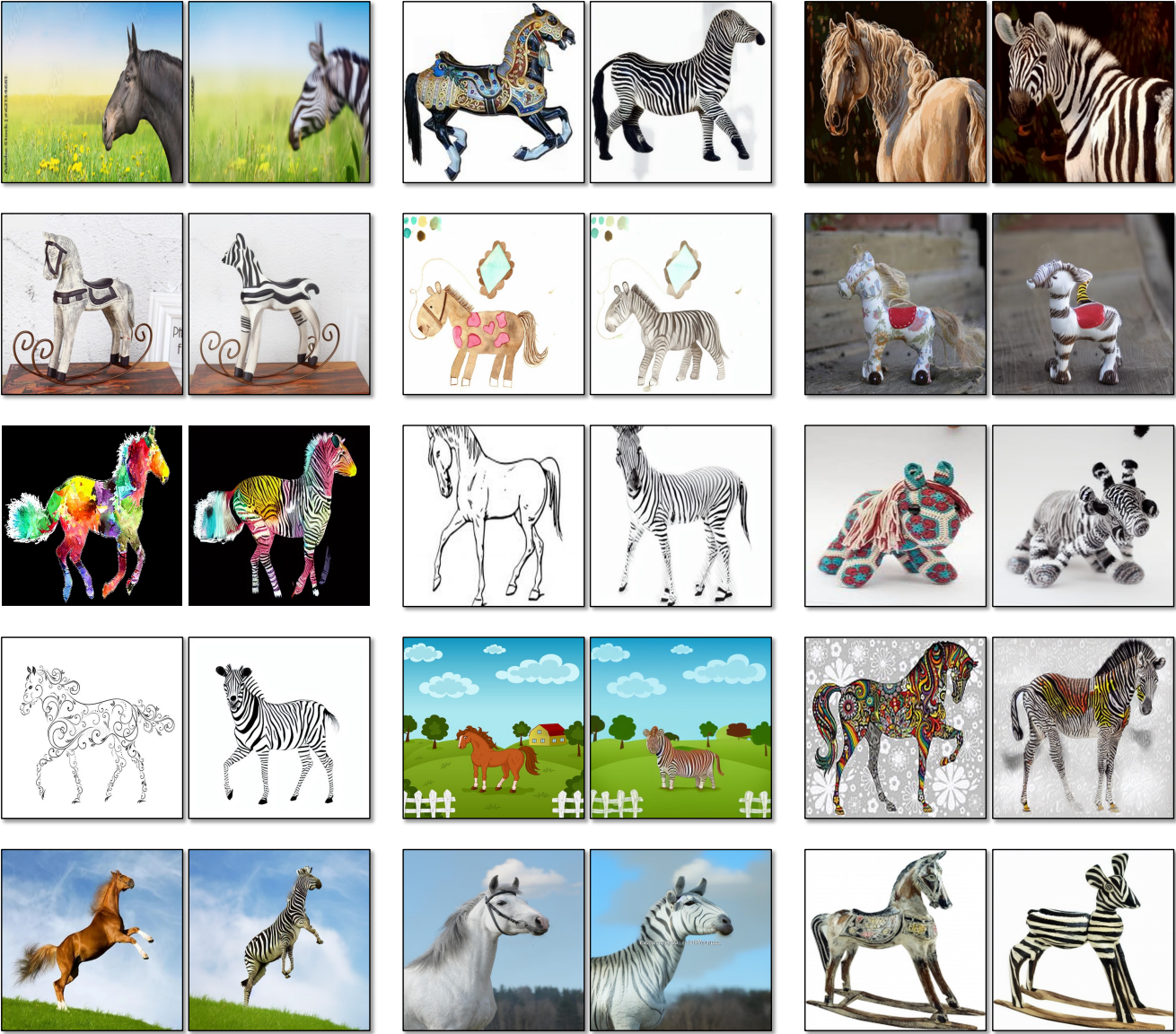


Figure 15: **Additional results.** We show additional results on real images for the horse → zebra task.

real image editing (zebra → horse)

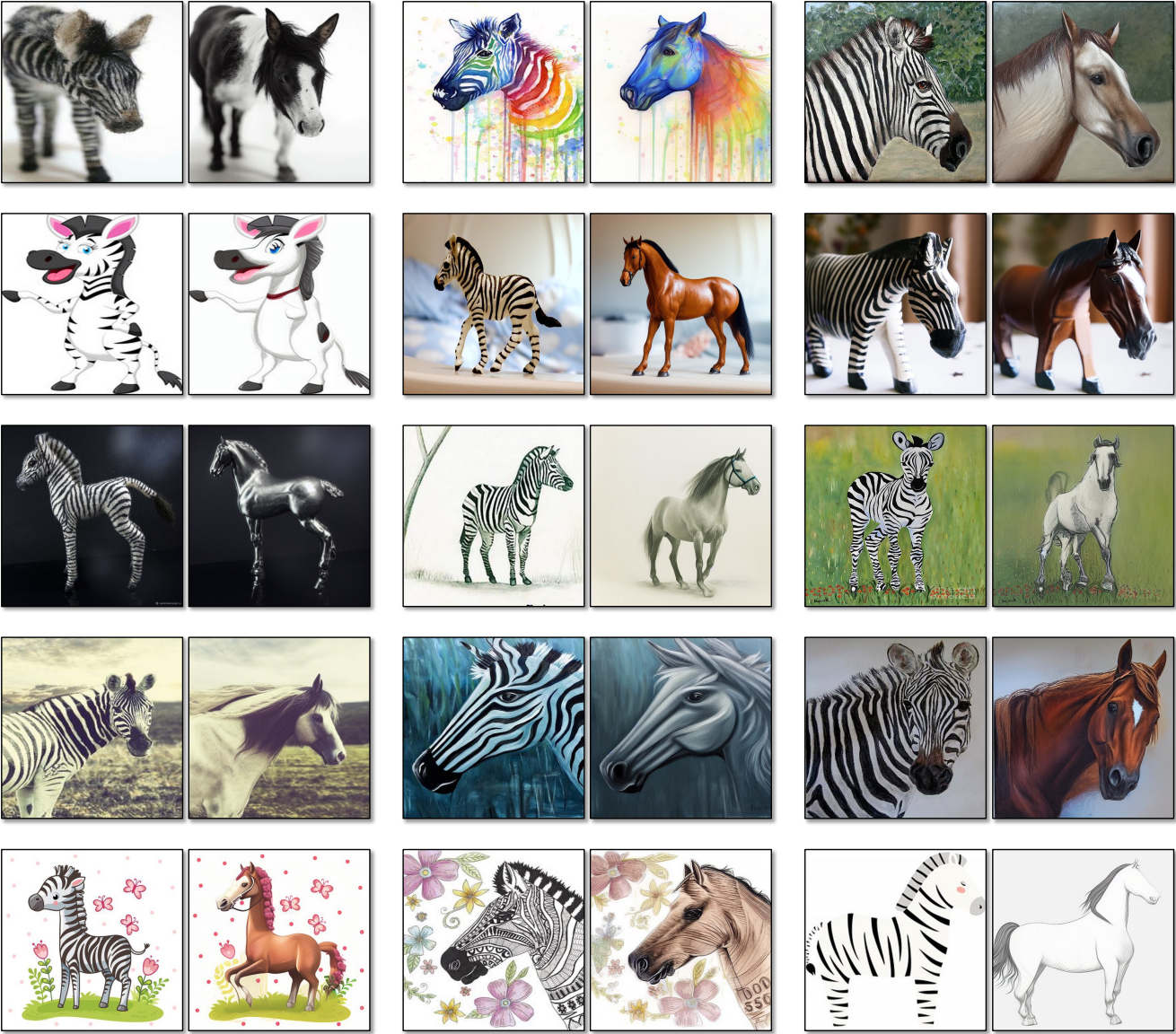


Figure 16: **Additional results.** We show additional results on real images for the zebra → horse task.